7-cell core hollow-core photonic crystal fibers with low loss in the spectral region around 2 mu m

Lyngsøe, Jens Kristian; Mangan, B.J.; Jakobsen, C.; Roberts, John

Published in:
Optics Express

Link to article, DOI:
10.1364/OE.17.023468

Publication date:
2009

Document Version
Publisher's PDF, also known as Version of record

7-cell core hollow-core photonic crystal fibers with low loss in the spectral region around 2 μm

J. K. Lyngsø,[1,2]* B. J. Mangan,[3] C. Jakobsen,[1] and P. J. Roberts[2]

[1]*NKT Photonics A/S, Blokken 84, DK-3460 Birkerød, Denmark*
[2]*DTU Fotonik, Technical University of Denmark, Ørsteds Plads 343, DK-2800 Kgs. Lyngby, Denmark*
[3]*University of Bath, Claverton Down, Bath BA2 7AY, United Kingdom*
**jkl@nktphotonics.com*

Abstract: Several 7 cell core hollow-core photonic crystal fibers with bandgaps in the spectral range of 1.4 μm to 2.3 μm have been fabricated. The transmission loss follows the $\approx \lambda^{-3}$ dependency previously reported, with a minimum measured loss of 9.5 dB/km at 1.99 μm. One fiber with a transmission loss of 26 dB/km at 2.3 μm is reported, which is significantly lower than the transmission loss of solid silica fibers at this wavelength.

OCIS codes: (060.5295) Photonic crystal fibers; (060.2390) Fiber optics, infrared.

References and links

1. P. J. Roberts, F. Couny, H. Sabert, B. J. Mangan, D. P. Williams, L. Farr, M. W. Mason, A. Tomlinson, T. A. Birks, J. C. Knight, and P. St. J. Russell, "Ultimate low loss of hollow-core photonic crystal fibres," Opt. Express **13**(1), 236 (2005).
2. Jas S. Sanghera, L. Brandon Shaw, and Ishwar D. Aggarwal, "Applications of chalcogenide glass optical fibers," C. R. Chim. **5**, 873–883 (2002).
3. J. Shephard, W. Macpherson, R. Maier, J. Jones, D. Hand, M. Mohebbi, A. George, P. Roberts, and J. Knight, "Single-mode mid-IR guidance in a hollow-core photonic crystal fiber," Opt. Express **13**(18), 7139–7144 (2005).
4. K. Saitoh, and M. Koshiba, "Leakage loss and group velocity dispersion in air-core photonic bandgap fibers," Opt. Express **11**(23), 3100–3109 (2003).
5. J. Limpert, T. Schreiber, S. Nolte, H. Zellmer, and A. Tünnermann, "All fiber chirped-pulse amplification system based on compression in air-guiding photonic bandgap fiber," Opt. Express **11**(24), 3332–3337 (2003).
6. V. N. Kumar, and D. N. Rao, "Using interference in the frequency domain for precise determination of thickness and refractive indices of normal dispersive materials," J. Opt. Soc. Am. B **12**(9), 1559–1563 (1995).
7. S. R. Nagel, J. B. MacChesney, and K. L. Walker, "An Overview of the Modified Chemical Vapor Deposition (MCVD) Process and Performance," IEEE J. Quantum Electron. **18**(4), 459–476 (1982).
8. D. Michel, V. B. Kazansky, and V. M. Andreev, "Study of the interaction between surface hydroxyls and adsorbed water molecules on porous glasses by means of infrared spectroscopy," Surf. Sci. **72**, 324–356 (1972).
9. J. Stone, and G. E. Walrafen, "Overtone vibrations of OH groups in fused silica optical fibers," J. Chem. Phys. **76**(4), 1712–1722 (1982).
10. P. S. Light, F. Couny, Y. Y. Wang, N. V. Wheeler, P. J. Roberts, and F. Benabid, "Double photonic bandgap hollow-core photonic crystal fiber," Opt. Express **17**(18), 16238–16243 (2009).
11. C. M. Smith, N. Venkataraman, M. T. Gallagher, D. Müller, J. A. West, N. F. Borrelli, D. C. Allan, and K. W. Koch, "Low-loss hollow-core silica/air photonic bandgap fibre," Nature **424**(6949), 657–659 (2003).
12. B. Mangan, J. K. Lyngsø, and P. J. Roberts, "Realization of Low Loss and Polarization Maintaining Hollow Core Photonic Crystal Fibers," in *Conference on Lasers and Electro-Optics/Quantum Electronics and Laser Science Conference and Photonic Applications Systems Technologies*, OSA Technical Digest (CD) (Optical Society of America, 2008), paper JFG4. *http://www.opticsinfobase.org/abstract.cfm?URI=CLEO-2008-JFG4*
13. P. J. Roberts, D. P. Williams, H. Sabert, B. J. Mangan, D. M. Bird, T. A. Birks, J. C. Knight, and P. St. J. Russell, "Design of low-loss and highly birefringent hollow-core photonic crystal fiber," Opt. Express **14**(16), 7329–7341 (2006).

1. Introduction

Hollow-core photonic crystal fibers (HC-PCF) guide light predominantly in a hollow core so that the overlap of the light field with silica is small compared to guidance in conventional solid silica fibers. As a consequence, the main contribution to the overall transmission loss is scattering of light at the air/silica interface inside the HC-PCF. The surface scattering loss dependency on wavelength was found to be proportional to λ^{-3} when it is understood that the fiber geometry being considered scales in proportion to the wavelength [1]. Furthermore,

#120080 - $15.00 USD Received 16 Nov 2009; accepted 30 Nov 2009; published 7 Dec 2009

because of the small overlap between silica and the light field, the infrared absorption is significantly reduced. Due to these effects, the minimum loss wavelength for standard 7-cell HC-PCFs is believed to be located around 2 μm [1].

Fiber lasers in the spectral region around 2 μm are of increasing interest because of promising applications in fields like spectroscopy, gas sensing and LIDAR systems. Due to the infrared absorption of silica, solid silica fibers are not suitable for transmission at wavelengths above 2 μm. Fibers made from materials with higher transmittance in this wavelength region, such as chalcogenide and fluoride glasses, have been developed [2]. Such fibers, however, suffer from higher non-linearity, increased fragility and are in general more difficult to handle than silica fibers. HC-PCFs are encouraging candidates for transmission of light in the short wavelength infrared region (1.4–3 μm). Previously, a silica 19-cell core HC-PCF has been demonstrated with a minimum loss of 2,600 dB/km at 3.14 μm [3]. The present study focuses on 7-cell core HC-PCFs, which, because of the smaller core, give rise to a slightly smaller fraction of the fundamental mode power propagating in air. They do, however, have the advantage of supporting fewer core modes than the 19-cell core HC-PCF, leading to more robust quasi single mode operation being possible with appropriate launch conditions.

The group velocity dispersion (GVD) of HC-PCFs is dominated by waveguide dispersion and evolves from normal to anomalous with increasing wavelength over the bandgap [4]. Accordingly, GVD can be tailored to be normal, zero or anomalous at a given wavelength by scaling the fiber dimensions. Anomalous GVD combined with the highly linearity of HC-PCFs has been utilized to demonstrate linear compression of positively chirped pulses in a HC-PCF at 1.04 μm [5]. Similarly, normal GVD in a HC-PCF around 2 μm can potentially be used for linear compression of negatively chirped pulses in a Thulium fiber laser setup.

2. Fiber fabrication

Five standard 7-cell core fibers were fabricated (Fibers A-E) using a conventional stack and draw technique. Each preform was built by stacking silica capillary tubes (Suprasil F300, Heraeus) in a hexagonal array making up the microstructured cladding. The 7-cell core was formed by removing 7 capillaries from the center of the structure and replacing them with a supporting silica core tube with identical wall thickness. The core size, cladding pitch and air filling fraction of the final fibers were controlled by carefully selecting the draw down ratio along with the core and cladding pressure during draw.

Table 1. Physical fiber dimensions

Fiber	Pitch [μm]	Core dia. [μm]
A	3.7	11.3
B	3.9	11.8
C	4.4	13.0
D	4.8	14.2
E	5.2	15.0
F	5.4	15.8

The fibers were drawn from different, but similar, preforms with the same basic design keeping the relative structure fixed and scaling the outside diameter to achieve the pitch listed in Table 1. The air filling fraction of the cladding structure was fixed at approximately 91% for all fibers. In addition, one 7-cell core fiber with antiresonant features on the core wall was fabricated (Fiber F) with a bandgap targeted at approximately 2 μm.

Figure 1 shows scanning electron micrographs of the end face of the fibers studied. Fibers A-E are standard 7-cell core HC-PCFs with a core wall thickness approximately equal to the cladding strut thickness and do not incorporate antiresonant features within the core wall. Fiber F is a similar 7-cell core HC-PCF but with antiresonant features on the core wall.

#120080 - $15.00 USD Received 16 Nov 2009; accepted 30 Nov 2009; published 7 Dec 2009

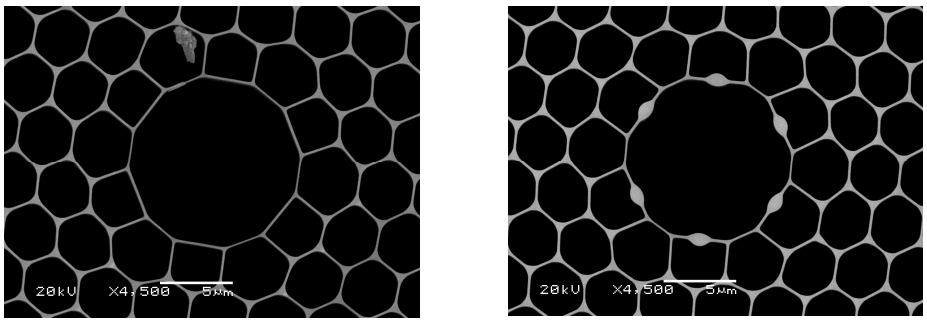

(a) **(b)**

Fig. 1. SEM images of the fiber designs used in this study. (a) The end face of a standard 7-cell core HC-PCF (Fibers A-E). All the fibers A,B,C,D and E have very similar geometry and vary only in scale. (b) The end face of a 7-cell core HC-PCF with six antiresonant features on the core wall (Fiber F).

3. Measurement technique and setup

The transmission loss was measured using a standard cut-back technique where at least three cleaves were performed on the output end of the full fiber length as well as on the cut-back section. Hence at least six scans per loss measurement were taken to quantify the measurement error. The minimum loss and the associated wavelength were recorded for each fiber along with the statistical uncertainty corresponding to one standard deviation. To measure the fundamental mode loss, at least 200 m. of cut-back section was used in order to strip the higher order modes (except fiber E and F, where a 50 m. cut-back section was used). An Ando AQ-4303B WLS was used as light source for fiber A and B, whereas a Koheras SuperK Compact was used for fiber C-F. The spectrum was recorded using a Yokogawa AQ6375 Optical Spectrum Analyzer with the spectral resolution set to 2 nm.

The group velocity dispersion of fiber E was measured with a low coherence Mach-Zehnder interferometer in the frequency domain as described in [6]. A Koheras SuperK Compact was used as light source and a Yokogawa AQ6375 Optical Spectrum Analyzer as the spectrometer.

4. General loss dependence on wavelength

In the explored spectral region, the general loss trend is dominated by surface scattering and infrared absorption. Hence only these contributions to the overall loss trend are considered, so that the overall loss is governed by [1]:

$$\alpha_t \approx \frac{S_0(f_a)}{\lambda^3} + A\exp(-a_{ir}/\lambda)(1-f_a) \qquad (1)$$

Where S_0 is the surface scattering coefficient, $A = 7.81 \times 10^{11}$ dB/km [7], $a_{ir} = -48.48$ μm [7] and f_a is the fraction of fundamental mode power propagating in air.

Figure 2(a) shows the measured minimum loss of each of the fibers A-E, together with the expected overall loss calculated from Eq. (1) with S_0 offset to match fiber A. The error bars correspond to one standard deviation. The solid grey line depicts the transmission loss of a conventional solid single mode fiber.

In the region above 1.9 μm the measured transmission loss for the 7-cell HC-PCFs is significantly lower than for solid silica fibers. The transmission loss of fiber E at 2.33 μm is approximately 26 dB/km compared to approximately 700 dB/km for a solid single mode fiber at this wavelength.

Figure 2(b) shows the fundamental mode loss as function of wavelength for fiber D. The structures at 1961 nm, 2009 nm and 2060 nm come from rotational states of CO_2 gas present

#120080 - $15.00 USD Received 16 Nov 2009; accepted 30 Nov 2009; published 7 Dec 2009

inside the fiber. The individual CO_2 rotational lines are averaged out in this plot due to the 2 nm resolution of the OSA.

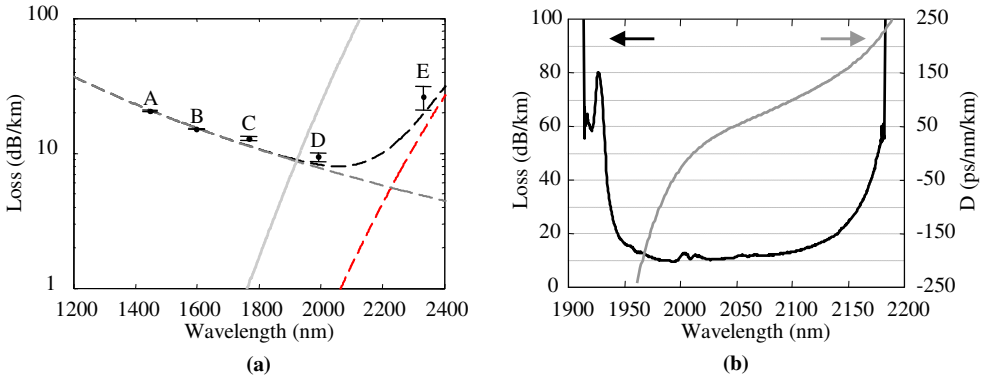

Fig. 2. (a) Measured minimum loss of fibers A-E, together with surface scattering loss (dashed grey), infrared absorption based on $f_a = 0.98$ (dashed red) and expected overall loss (dashed black). The solid grey line is the loss of a conventional solid single mode fiber. (b) Fundamental mode loss as function of wavelength for fiber D (black) and group velocity dispersion (grey).

The GVD of fiber D is plotted along side the transmission loss in Fig. 2(b). This specific fiber exhibits a zero dispersion wavelength at $\lambda_0 \approx 2010$ nm and a dispersion slope of $S_0 \approx 2.4$ ps/nm^2/km at this wavelength.

5. Excess loss

In the region between 1.6 μm and 2.4 μm, several sources of absorption loss were observed. At 1896 nm, a strong absorption probably caused by molecular water adsorbed on the silica surface [8] was apparent, and at 2210 nm, an absorption caused by the $\nu_4(OH) + \nu_3(SiO_2)$ combination vibration was observed [9].

The atmosphere inside the fibers unintentionally contains gases originating either from the silica glass itself or from the fabrication process. Ro-vibrational spectra caused by HCl and CO_2 were identified in the transmission spectra of the fibers, taken with the spectral resolution of the OSA set to 0.05 nm. Figure 3(a) shows the transmission of fiber D, where the spectrum caused by CO_2 gas was observed. Figure 3(b) shows a similar example, this time for fiber C, where a HCl gas spectrum was observed. These excess loss mechanisms contributed to the overall measured loss leading to a somewhat higher than expected transmission loss of fibers C-E. CO_2 is believed to originate from the fabrication process and thus should be relatively easy to remove. HCl, on the other hand, comes from constituents intrinsic to the fused silica used to build the preforms and therefore is more challenging to eliminate.

#120080 - $15.00 USD Received 16 Nov 2009; accepted 30 Nov 2009; published 7 Dec 2009

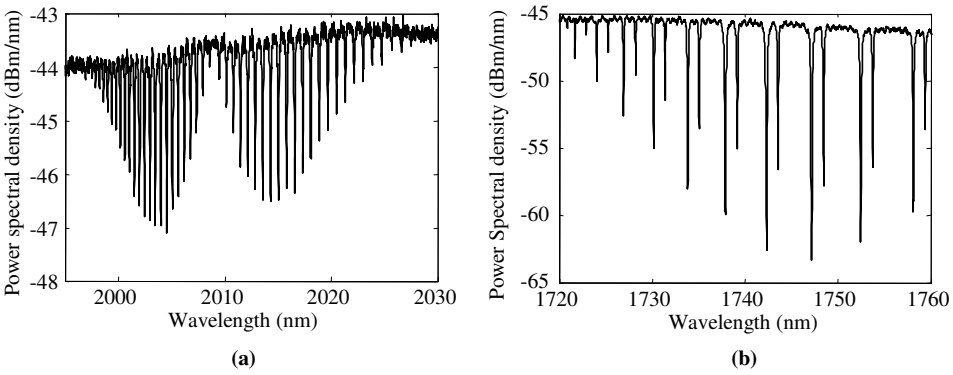

Fig. 3. (a) Ro-vibrational spectrum originating from CO_2 present inside the fiber. Signal corresponds to transmission through 200 m. fiber. (b) The P branch of the ro-vibrational spectrum originating from HCl present inside the fiber. Signal corresponds to transmission through 400 m. fiber.

6. Second order bandgap

For a typical HC-PCF cladding geometry at 91% air filling fraction, a weak second order bandgap opens up in addition to the stronger "fundamental" bandgap responsible for the robust guiding studied above. The cladding photonic density of states was calculated by a finite element frequency domain method using Bloch-periodic boundary conditions on a unit cell of the cladding. Figure 4(a) shows the calculated photonic density of states where white corresponds to a region with several guided cladding states and black corresponds to no cladding states being allowed. Thus black regions are photonic bandgaps where light can be guided in the core. As can be seen from Fig. 4(a) the "fundamental" bandgap is centered on a normalized wavenumber $k\Lambda \approx 15$ whereas the second order bandgap is located around $k\Lambda \approx 22$. This means that for fiber E with $\Lambda \approx 5.2$ μm, this higher order bandgap is located in the telecom wavelength region making it potentially suitable as a pump guide. Close to a normalized wavenumber $k\Lambda = 20$, the cladding photonic density of states is low, but it does not completely vanish and we did not observe any core guided modes in this region.

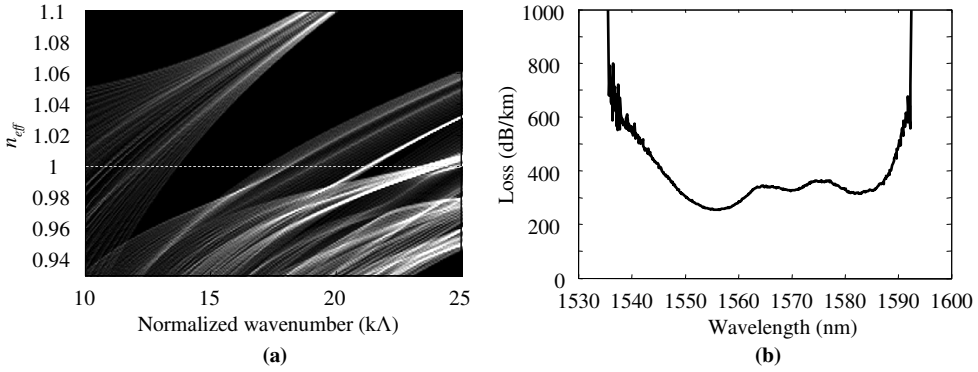

Fig. 4. (a) Photonic density of states for a typical HC-PCF cladding with a 91% air filling fraction. Black regions correspond to no cladding states being allowed. (b) Measured loss of the first higher order bandgap of fiber E.

Figure 4(b) is a plot of the measured transmission loss in the higher order bandgap of Fiber E. As reported in [10], the loss in this higher order bandgap is significantly higher than the loss for guidance in the fundamental bandgap (Fiber B). Our calculations show that the leakage loss of the HE_{11}-like core mode in this bandgap is approximately four orders of

#120080 - $15.00 USD Received 16 Nov 2009; accepted 30 Nov 2009; published 7 Dec 2009

magnitude higher than when in the fundamental bandgap. From the cladding photonic density of states plot it can be seen that the higher order bandgap is approximately 100 nm wide. Since a large number of surface states reside either side of the bandgap, and structural imperfections occur in the fabricated fibers, an effective bandwidth of around 50 nm was observed experimentally.

7. Antiresonant features on the core wall

Placing antiresonant features on the core wall reduces the overlap between the guided light field and silica [11–13]. This causes a reduction of both the surface scattering loss and the silica infrared absorption compared to the standard 7-cell core HC-PCF. Figure 5(a) shows the overall loss with S_0 offset to match fibers with antiresonant features in the core wall recently reported [12], together with fiber F which had a defect in the cladding structure near the core. The defect caused a distortion of the bandgap at the short wavelength edge and possibly also led to the slightly higher than expected loss – see Fig. 5(b).

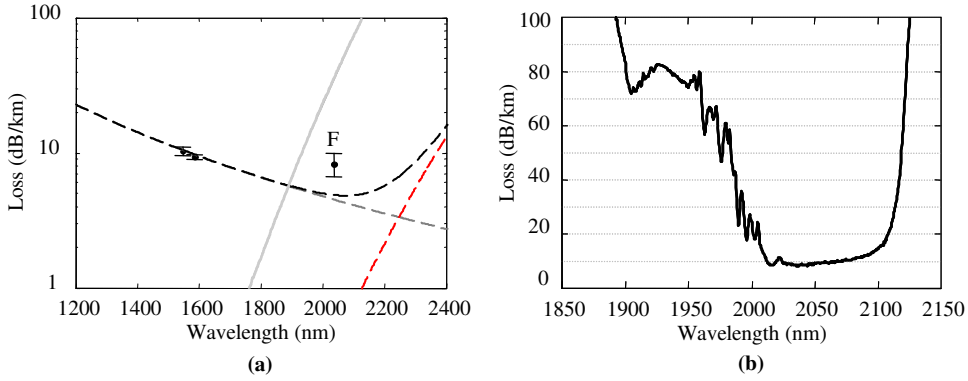

Fig. 5. (a) Measured loss for 7-cell core HC-PCFs with antiresonant features on the core wall, together with surface scattering loss (dashed grey), infrared absorption based on f_a = 0.99 (dashed red) and expected overall loss (dashed black). (b) Fundamental mode loss as function of wavelength for fiber F. There was a defect in the cladding structure near the core.

8. Conclusions

Five standard 7-cell core HC-PCFs have been fabricated and characterized with photonic bandgaps in the region between 1.4 μm and 2.3 μm. The overall loss dependence on wavelength agrees with previously reported results, with the lowest measured transmission loss being 9.5 dB/km at 1.99 μm. A fiber with a transmission loss of 26 dB/km at 2.3 μm has been reported, which is significantly lower than the transmission loss of solid silica fibers at this wavelength. In addition, a 7-cell core HC-PCF with antiresonant features on the core wall has been fabricated with a minimum loss of 8 dB/km at 2.03 μm. The fibers have proven to be effective gas cells for observing ro-vibrational spectra of gases such as HCl and CO_2.

#120080 - $15.00 USD Received 16 Nov 2009; accepted 30 Nov 2009; published 7 Dec 2009